

Compression mechanism of brucite: An investigation by structural refinement under pressure

T. NAGAI,* T. HATTORI, AND T. YAMANAKA

Department of Earth and Space Science, Osaka University, Toyonaka, Osaka 560-0043, Japan

ABSTRACT

Synchrotron X-ray powder diffraction study of brucite, $\text{Mg}(\text{OH})_2$, was carried out in a diamond anvil cell with an imaging plate detector from 0.6 to 18.0 GPa at room temperature using the angular-dispersive technique on beamline BL-18C at the Photon Factory, KEK, Japan. Using Rietveld analysis, unit-cell parameters as well as atomic positions of the O atoms in brucite have been successfully refined, taking into account the effects of preferred orientation. Variation of the c/a ratio with pressure indicates that the compression mechanism changes around 10 GPa, above which the compression behavior is isotropic. Based on the changes of the refined atomic positions of the O atoms with pressure, we conclude that the shortening of the interlayer distance controls compression below 10 GPa, whereas above this pressure compression of the oxygen sublattice is the dominant mechanism. Results of the structural refinements also suggest that the MgO_6 octahedral regularity initially approaches a regular configuration with pressure, which then remains unchanged above 10 GPa.

INTRODUCTION

Brucite, $\text{Mg}(\text{OH})_2$, has the CdI_2 -type structure (trigonal, space group $P3m1$), with layers of MgO_6 octahedra stacked along the c axis. Each O atom is hydrogenated with the O-H bond along the threefold axis above and below the octahedral layers.

Many previous studies have discussed the compression behavior through the change of unit-cell parameters under pressure (Fei and Mao 1993; Catti et al. 1995; Duffy et al. 1995a; Xia et al. 1998). However, a large amount of scatter exists among the equation of state parameters for brucite derived from various compression studies because brucite is strongly anisotropic and the compression behavior is often affected by preferred orientation and deviatoric stresses in the sample. Previous studies suggested a change of compression mechanism at high pressure, based on the variation of the c/a ratio with pressure (Fei and Mao 1993; Duffy et al. 1995a; Xia et al. 1998). It has been reported that the linear compressibilities along the a and c axes become comparable above about 10 GPa, although the c axis should be more compressible from the crystallographic view point (Xia et al. 1998). Catti et al. (1995) reported a discontinuous change in the c/a ratio at 6–7 GPa and interpreted it as a second-order phase transition, such as the disordering of the H atoms. In contrast, other diffraction studies did not detect such discontinuity (Fei and Mao 1993; Duffy et al. 1995a; Xia et al. 1998). The detail of the compression mechanism remains unclear and it is difficult to understand the mechanism based on the pressure dependency of unit-cell parameters alone.

Neutron diffraction and spectroscopic studies have indicated that brucite undergoes pressure-induced disordering of the H atoms below 10 GPa (Kruger et al. 1990; Parise et al. 1994; Catti et al. 1995). A recent polarized IR spectroscopic study suggested the pressure-induced proton transfer in brucite (Shinoda and Aikawa 1998). No information exists as to whether the H atoms disordering could influence the configuration of the octahedral layers.

The use of an imaging-plate (IP) area detector has greatly improved the quality of diffraction data from powder samples pressurized in a diamond anvil cell (DAC). Its combination with synchrotron radiation provides a powerful tool in the high-pressure diffraction study. The high-quality angular-dispersive diffraction patterns thus obtained at high pressures allow us to more accurately determine the unit-cell parameters, and to refine the atomic positions through Rietveld analysis (Shimomura et al. 1992; Fujihisa et al. 1992), instead of structural refinement by energy-dispersive profile fitting (Yamanaka and Ogata 1991). Based on the results of these reliable refinements, we discuss the compression mechanism of brucite.

EXPERIMENTAL METHODS

Procedures

Reagent-grade $\text{Mg}(\text{OH})_2$ powder samples [$a = 3.1425(2)$ Å, $c = 4.7665(3)$ Å, $V = 40.746(2)$ Å³] were compressed in a lever-and-spring type DAC. Because brucite dissolves in a conventional 4:1 methanol/ethanol pressure medium under pressure, silicon oil was used as pressure medium (Andraut and Poirier 1991; Yano et al. 1994; Petit et al. 1996). A pair of 450 μm culet diamonds and a preindented stainless steel gasket were used. The size of the sample chamber was about 200-

*E-mail: nagai@ess.sci.osaka-u.ac.jp

μm in diameter and $80\ \mu\text{m}$ thick. Small ruby chips were also placed in the sample chamber as a pressure calibrant. All angular-dispersive synchrotron X-ray diffraction experiments were performed on the BL-18C beamline at the Photon Factory using an imaging plate (IP) detector. The monochromatized incident beam was tuned to an energy of 20 keV and is collimated to $80\ \mu\text{m}$ in diameter (Kikegawa 1997). Typical exposure time was an hour.

Analysis

The two-dimensional image was integrated along each Debye-Scherrer ring and converted to a one-dimensional diffraction pattern by using the program PIP (Powder pattern analyzer for Imaging Plate) (Fujihisa and Aoki 1998). The scattering-angle dependence of the absorption factor of the DAC was corrected in consideration of X-ray path in the DAC, but the absorption factor due to samples was not corrected, because its value is negligible. After the absorption correction, we carried out a Rietveld analysis using the program RIETAN (Izumi 1993). The Mg atoms in the structure of brucite occupy a special position, 1a site at (0,0,0), and the O and H atoms occupy the 2d site at ($1/3, 2/3, z_0$). The experimental accuracy is insufficient to allow refinement of H atom positions because the scattering power of the H atom is negligibly small for X-rays. Therefore, only the fractional z coordinate of the O atom (z_0) was refined. Several cycles of least-squares calculation carried out to adjust the unit cell, background, and peak width parameters before refining the atomic position of the O atom. A preferred orientation parameter was also refined, because it is important to evaluate the effect of preferred orientation on a highly anisotropic structure. Preferred orientation was corrected by using the March-Dolase function in the program RIETAN. For samples exhibiting no preferred orientation, the preferred orientation parameter, r , is equal to one. Diffraction data at high Bragg angles are needed to refine reliably thermal parameters, which are of course the most sensitive to systematic errors; however, it is difficult to collect diffraction patterns up to sufficient high Bragg angles in the current DAC experiments, because of its geometrical constrains. Therefore, isotropic thermal parameters, $B/\text{\AA}^2$, for Mg and O were refined to be 0.48(3) and 0.82(4), respectively, for the data obtained at 0.6 GPa and were fixed in the refinements of data at higher pressures. An ex-

ample of a Rietveld refinement result is shown in Figure 1. All results are in Table 1.

RESULTS AND DISCUSSION

The change of the a axis as a function of pressure (Fig. 2) is comparable to that reported in previous studies, but the c axis is a little stiffer in our studies (Fei and Mao 1993; Catti et al. 1995; Duffy et al. 1995a; Xia et al. 1998). Variations of the c/a ratio and unit-cell volume with pressure (Fig. 2) show a gentler slope than those from previous studies. We attribute this difference to both deviatoric stresses in a DAC and preferred orientation of the sample in some experiments. Brucite powder in the DAC is apt to show a significant preferred orientation, with the c axis tending to align along the axis of the DAC, and in this case, the stress along the axis of compression would be larger than that in the radial direction, especially above the solidification pressure of the pressure medium (Singh and Balasingh 1994). With the geometry of our X-ray diffraction experiment, where the axis of the DAC is parallel to the incident X-ray, a preferred orientation would lead to systematic underestimation of the c dimension and lower c/a values (Duffy et al. 1995a). However, the refined preferred orientation parameter, r , was almost constant at 1.1(1), which indicates that

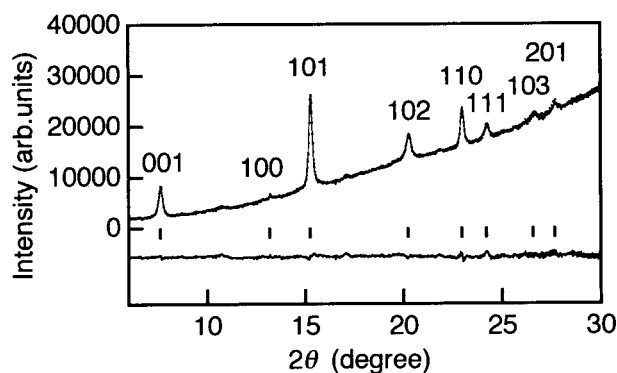


FIGURE 1. Observed (dots) and calculated (solid line) profile of brucite at 2.5 GPa. Differences between the observed and calculated intensities are plotted at the bottom and vertical bars represent the positions of the diffraction peaks. The increase in the background at high angles seems to be due to Compton scattering of diamonds.

TABLE 1. Rietveld refined atomic parameters and selected interatomic distances (Å) and angles ($^\circ$) of brucite

P (GPa)	0.6	2.5	6.2	8.9	12.5	16.0	18.0
a (Å)	3.1264(2)	3.1090(3)	3.0763(5)	3.0553(6)	3.0114(7)	3.0003(8)	2.9838(8)
c (Å)	4.7315(5)	4.6573(7)	4.549(1)	4.475(1)	4.353(1)	4.325(2)	4.294(2)
V (Å ³)	40.05(1)	38.98(6)	37.28(2)	36.13(2)	34.19(1)	33.72(3)	33.11(2)
z_0	0.220(1)	0.226(1)	0.235(2)	0.246(2)	0.250(2)	0.246(3)	0.250(2)
R_{wp}^*	2.23	1.96	2.77	1.99	1.91	2.34	1.81
R_p^*	1.32	1.45	1.88	1.53	1.40	1.64	1.14
RB^*	6.53	5.63	7.69	4.81	6.57	4.58	4.92
Octa. thick	2.082(3)	2.111(4)	2.14(2)	2.20(2)	2.18(3)	2.13(2)	2.15(4)
Interlayer	2.651(3)	2.552(2)	2.41(2)	2.27(2)	2.18(4)	2.20(4)	2.15(3)
Mg-O $\times 6$	2.084(4)	2.081(5)	2.07(1)	2.08(1)	2.05(1)	2.03(1)	2.03(1)
O-Mg-O	97.2(2)	96.7(1)	95.8(2)	94.5(4)	94.5(4)	95.1(3)	94.6(3)
O...O \dagger	3.206(1)	3.120(2)	3.00(1)	2.88(2)	2.80(3)	2.80(2)	2.75(2)
$r\ddagger$	1.122(8)	1.10(2)	1.12(2)	1.10(2)	1.18(2)	1.18(2)	1.18(2)

* See Young et al. (1982) for definitions of the discrepancy indices.

\dagger Interlayer O...O distances.

\ddagger See Izumi (1993) for a definition of the preferred orientation parameter.

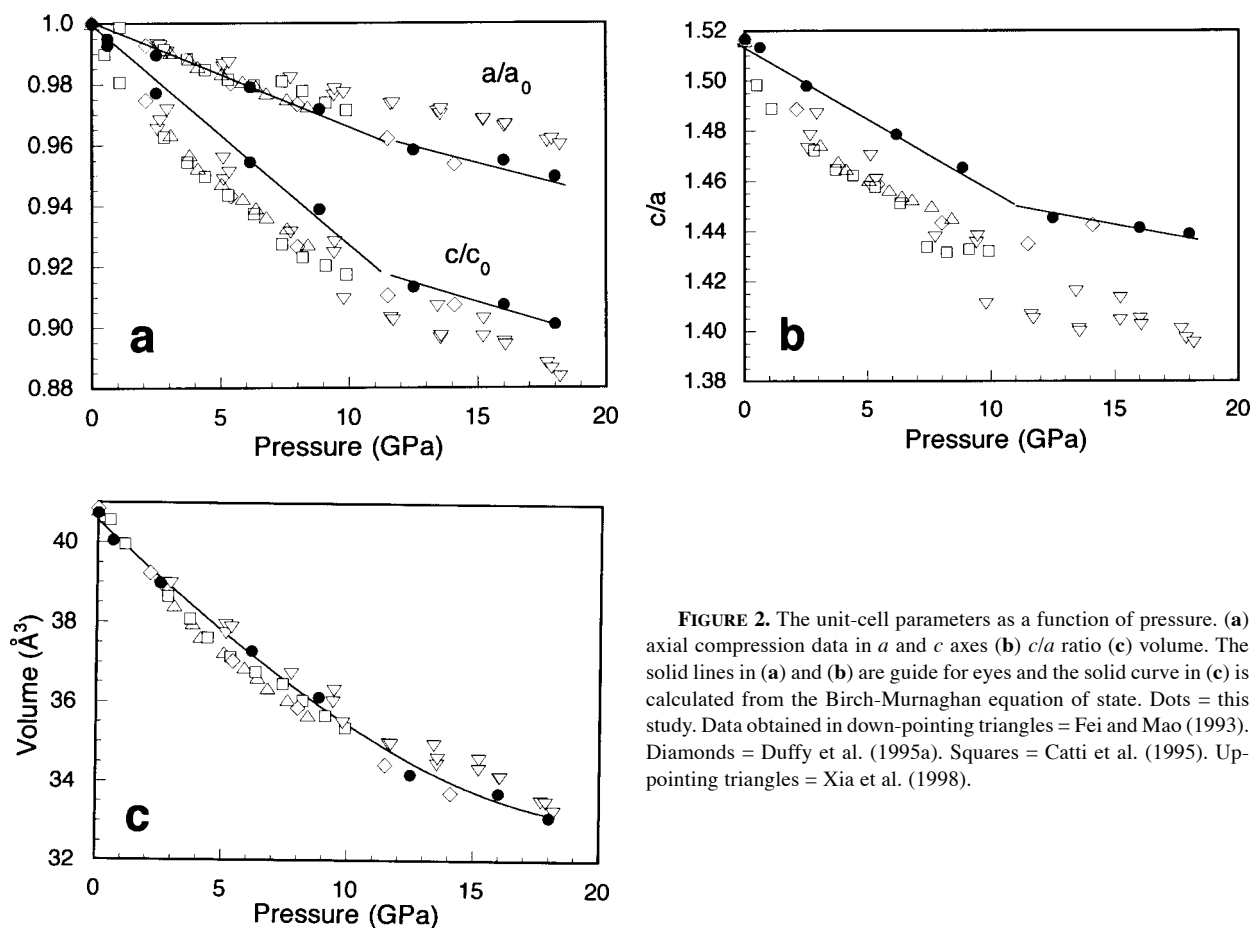


FIGURE 2. The unit-cell parameters as a function of pressure. (a) axial compression data in a and c axes (b) c/a ratio (c) volume. The solid lines in (a) and (b) are guide for eyes and the solid curve in (c) is calculated from the Birch-Murnaghan equation of state. Dots = this study. Data obtained in down-pointing triangles = Fei and Mao (1993). Diamonds = Duffy et al. (1995a). Squares = Catti et al. (1995). Up-pointing triangles = Xia et al. (1998).

preferred orientation is negligible in this study. In fact, we could observe the 001 reflection with sufficient intensity under pressure and our study obtained higher c/a values than those in previous studies. Therefore, reliability of the result has been significantly increased in this study by the quantitatively evaluated preferred orientation and full spectrum analysis.

The pressure dependence of the linear compressibilities of the a and c axes is quite different (Fig. 2). The a axis is almost linearly compressed in all range of experimental pressure, whereas the c axis is linearly compressed up to about 10 GPa. Above this pressure, the compressibility of the c axis becomes smaller and comparable to that of the a axis above the pressure. Consequently, the c/a ratio initially decreases rapidly with pressure but then the slope becomes smaller above about 10 GPa. This change of the linear compressibilities of the a and c axes indicates that the compression behavior changes from highly anisotropic to almost isotropic at higher pressures. Some previous studies also reported the similar slope change of the c/a ratio decreasing with pressure (Fei and Mao 1993; Duffy et al. 1995a; Xia et al. 1998).

The peak widths (Fig. 3) increase with P up to about 8 GPa, above which the values remain constant. Peaks are broadened by a factor of 5 at 8.9 GPa. This is presumably due to microscopic deviatoric stress resulted from solidification of the sili-

con oil pressure medium. This may partly be responsible for the observed changes in unit-cell dimensions. However, further experimental works is needed to exclude microscopic deviatoric stress effects. Catti et al. (1995) reported a sharp drop of the c/a ratio at about 7 GPa, but our data of unit-cell parameters do not show such sharp discontinuity. The bulk modulus (K_{70}) was determined as 44(1) GPa from the least-squares fit to the third-order Birch-Murnaghan equation of state, which assumes $K' = 6.7$. For comparison, Xia et al. (1998) reported $K_0 = 39.69(14)$ GPa and $K' = 6.7(7)$ from a third-order Birch-Murnaghan equation of state fit to the data obtained by the improved stress controlled experiments.

Previous X-ray diffraction studies have discussed the compression behavior only from the pressure dependence of unit-cell parameters. One important feature of our study is that the structure refinement by Rietveld analysis enables us to discuss the compression mechanism from the crystallographic view point of the atomic displacement. The variation of the fractional z coordinate of the O atom (z_0) with pressure (Fig. 4) is in good agreement with the data obtained by neutron powder diffraction experiments by Catti et al. (1995). The value of z_0 initially increases linearly up to 0.25 with pressure, but then remains constant at 0.25 above 10 GPa. The thickness of the interlayer ($2 \times z_0 \times c$) and MgO_6 octahedral layer ($c - 2 \times z_0 \times c$)

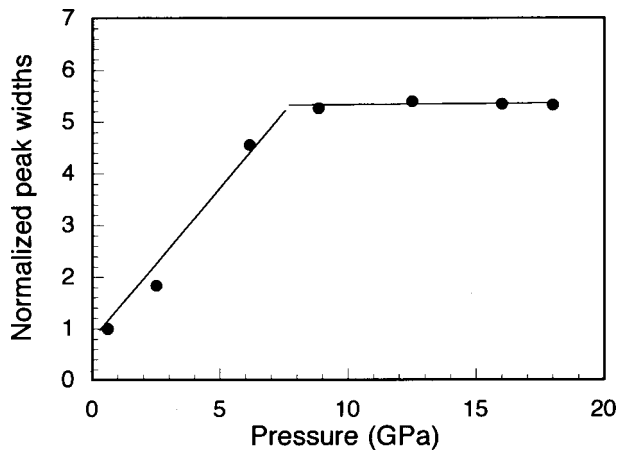


FIGURE 3. Peak widths (FWHM) normalized by the value at 0.6 GPa as a function of pressure. Errors are about the size of the symbols.

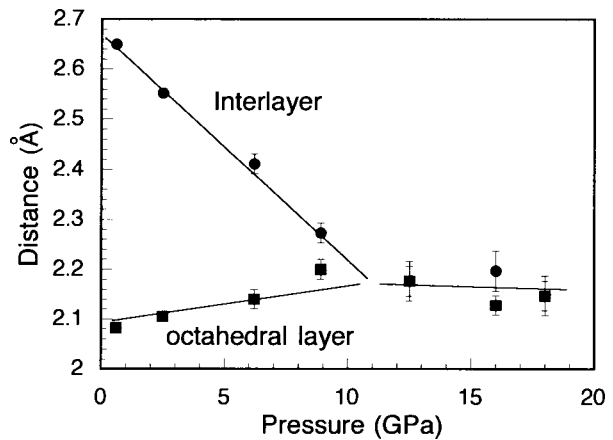


FIGURE 5. The thickness of the interlayer (dots) and octahedral layer (squares) in brucite as a function of pressure.

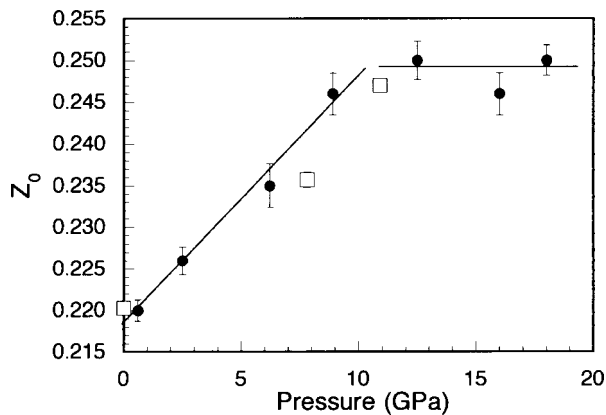


FIGURE 4. Variation of the fractional z coordinate, z_0 , of the O atoms as a function of pressure. The solid lines are guide for eyes. The open squares represent neutron data of Catti et al. (1995).

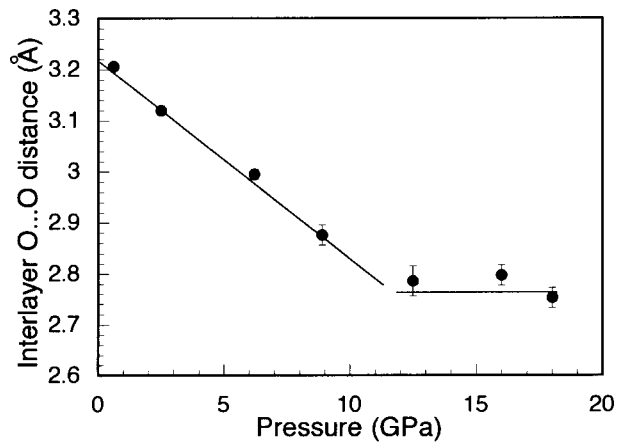


FIGURE 6. Variation of the interlayer O...O distance as a function of pressure.

in brucite can be easily calculated from the value of z_0 and the c axis dimension (Fig. 5). Although the thickness of octahedral layer slightly increases with pressure, the interlayer thickness decreases by about 19% up to 10 GPa. From the crystallographic constraints in the brucite structure, the shortening of the Mg-O distance should lead to decrease of octahedral layer thickness, whereas, the decrease of the O-Mg-O angle will cause the thickness to increase. Below 10 GPa, the shortening of the Mg-O distance is slight (0.01 Å at most) and the O-Mg-O angle decreases from 97.3° to 94.5° (Fig. 6). Consequently, octahedral layer thickness increases slightly for pressure range up to 10 GPa. The increase of octahedral thickness does not mean that the volume of the MgO₆ octahedron expands with pressure. Above 10 GPa, the interlayer and the octahedral layer have the same thickness, because the value of z_0 becomes almost a constant with an ideal value of 0.25. In addition, the Mg-O distance decreases faster than below 10 GPa and the O-Mg-O angle remains almost constant at 94.5°. This information indicates that the shortening of the interlayer distance is the dominant

compression mechanism below 10 GPa and that the compression of the oxygen sublattice is dominant mechanism above 10 GPa. This change in mechanism can explain the change of the compression behavior from highly anisotropic to almost isotropic, as seen from the slope change of the c/a ratio at about 10 GPa. Furthermore, the O-Mg-O angle directly represents the octahedral regularity in the brucite structure. The decrease of the O-Mg-O angle below 10 GPa indicates that the MgO₆ octahedron approaches to the regular configuration. However, above 10 GPa, the O-Mg-O angle remains almost constant, which indicates that the octahedral regularity of MgO₆ octahedron shows no more change above the pressure.

Previous neutron diffraction and spectroscopic studies reported pressure-induced H bonding in brucite at about 5 GPa (Parise et al. 1993, Duffy et al. 1995b; Catti et al. 1995; Shinoda and Aikawa 1998). The effect of the formation of H bonding does not seem to affect the compression behavior nor the Mg-O sublattice, because present data does not show any discontinuity in either unit-cell change or the atomic displacement at about 5 GPa.

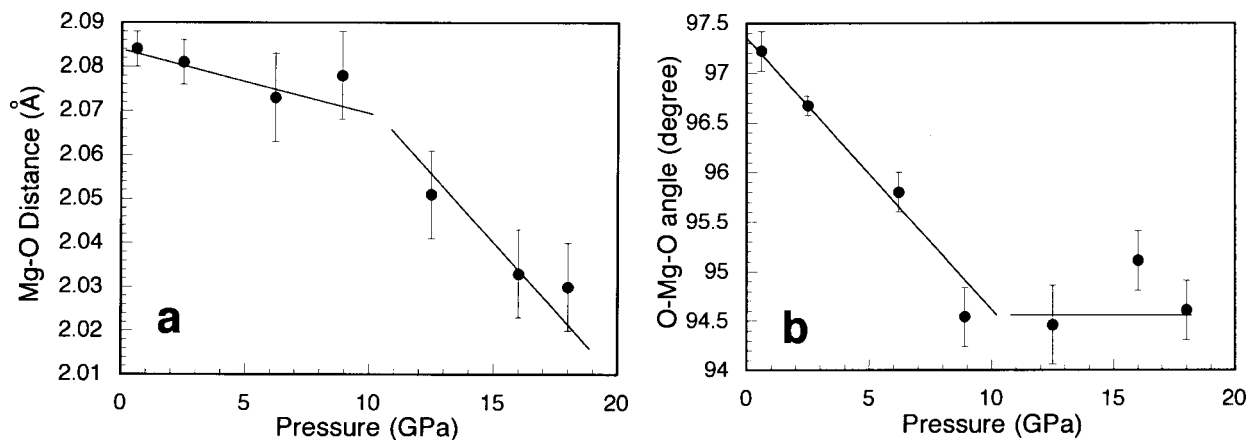


FIGURE 7. Variation of (a) the Mg-O distance and (b) the O-Mg-O angle in a MgO₆ octahedra as a function of pressure.

Martens and Freund (1976) suggested that the shortening of the interlayer O··O distance enhances proton transfer from donors to acceptors of O atoms. Indeed, Shinoda and Aikawa (1998) explained the pressure dependence of IR absorbency by the increasing proportion of proton transfer between interlayers with pressure. Interlayer O··O distance is shown as a function of pressure in Figure 7. The interlayer O··O distance initially decreases monotonically with pressure, but appears to be saturated at about 2.75 Å above 10 GPa. The shortening of the interlayer O··O distance may enhance the H bonding, but simultaneously the shortening must cause the repulsion between the donor and acceptor of O atoms (Brown 1995). Both repulsion and the strength of the H bonding are considered to keep their balance. The saturated value of the interlayer O··O distance of 2.75 Å may represent a limit of the stable balance in brucite between the repulsion and the strength of the H bonding under pressure. This balance would lead to the change of the compression mechanism at about 10 GPa.

ACKNOWLEDGMENTS

We are grateful to T. Kikegawa and Y. Murai for their help in the X-ray diffraction experiments at PF. We also thank H. Fujihisa for providing the program PIP and T. Ito for assistance of its installation. Y. Wang and two anonymous reviewers are greatly acknowledged for helpful and constructive reviews. The X-ray diffraction studies at BL-18C in PF were performed under the approval of the Photon Factory Advisory Committee (proposal no. 97-G270). This work was partly supported by Grant-in-Aid for Scientific Research (No. 10640463) from the Ministry of Education of Japan.

REFERENCES CITED

- Andraut, D. and Poirier, J.P. (1991) Evolution of the distortion of perovskite under pressure: an EXAFS study of BaZrO₃, SrZrO₃, and CaGeO₃. *Physics and Chemistry of Minerals*, 18, 91–105.
- Brown, I.D. (1995) Anion-anion repulsion, coordination number, and the asymmetry of hydrogen bonds. *Canadian Journal of Physics*, 73, 676–682.
- Catti, M., Ferraris, G., Hull, S., and Pavese, A. (1995) Static compression and H disorder in brucite, Mg(OH)₂, to 11 GPa: a powder neutron diffraction study. *Physics and Chemistry of Minerals*, 22, 200–206.
- Duffy, T.S., Shu, J., Mao, H.K., and Hemley, R. (1995a) Single-crystal x-ray diffraction of brucite to 14 GPa. *Physics and Chemistry of Minerals*, 22, 277–281.
- Duffy, T.S., Meade, C., Fei, Y., Mao, H.K., and Hemley, R. (1995b) High-pressure phase transition in brucite, Mg(OH)₂. *American Mineralogist*, 80, 222–230.
- Fei, Y. and Mao, H.K. (1993) Static compression of Mg(OH)₂ to 78 GPa at high temperature and constraints on equation of state of fluid H₂O. *Journal of Geophysical Research*, 98, 11875–11884.
- Fujihisa, H. and Aoki, K. (1998) High pressure x-ray powder diffraction experiments and intensity analyses. *The Review of High Pressure Science and Technology*, 8, 4–9.
- Fujihisa, H., Fujii, Y., Sakata, M., Takata, M., Kubota, Y., Takemura, K., and Shomomura, O. (1992) Electron density distribution in solid iodine refined by maximum entropy method. In A.K. Singh, Ed., *Recent Trends in High Pressure Research*, p. 145–147. Oxford and IBH Publishing Company, New Delhi.
- Izumi, F. (1993) Rietveld analysis programs RIETAN and PREMOS and special applications. In R.A. Young, Ed., 298 p. Oxford University Press, Oxford.
- Kikegawa, T. (1997) Photon Factory Activity Report, High Energy Accelerator Research Organization, KEK, Tsukuba, 113.
- Kruger, M.B., Williams, Q., and Jeanloz, R. (1989) Vibrational spectra of Mg(OH)₂ and Ca(OH)₂ under pressure. *Journal of Chemical Physics*, 91, 5910–5915.
- Martens, R. and Freund, F. (1976) The potential energy curve of proton and the dissociation energy of the OH⁻ ion in Mg(OH)₂. *Physica Status Solidi (A)* 37, 97–104.
- Parise, J.B., Leinenweber, K., Weidner, D.J., Tan, K., and Von Dreels, R.B. (1994) Pressure-induced H bonding: neutron diffraction study of brucite, Mg(OH)₂, to 9.3 GPa. *American Mineralogist*, 79, 193–196.
- Petit, P.E., Guyot, F., Fiquet, G., and Itie, J.P. (1996) High-pressure behavior of germanate olivines studied by X-ray diffraction and X-ray absorption spectroscopy. *Physics and Chemistry of Minerals*, 23, 173–185.
- Shimomura, O., Takemura, K., Fujihisa, H., Fujii, Y., Ohishi, Y., Kikegawa, T., Amemiya, Y., and Matsushita, T. (1992) Application of an imaging plate to high-pressure x-ray study with a diamond anvil cell. *Review of Science and Instrument*, 63, 967–973.
- Shinoda, K. and Aikawa, N. (1998) Interlayer proton transfer in brucite under pressure by polarized IR spectroscopy to 5.3 GPa. *Physics and Chemistry of Minerals*, 25, 197–202.
- Singh, A.K. and Balasingh, C. (1994) The lattice strains in an opposed anvil high pressure setup. *Journal of Applied Physics*, 75, 4956–4962.
- Xia, X., Weidner, D.J., and Zhao, H. (1998) Equation of state of brucite: Single-crystal Brillouin spectroscopy study and Polycrystalline pressure-volume-temperature measurement. *American Mineralogist*, 83, 68–74.
- Yamanaka, T. and Ogata, K. (1991) Structure refinement of GeO₂ polymorphs at high pressures and temperatures by energy dispersive spectra of powder diffraction. *Journal of Applied Crystallography*, 24, 111–118.
- Yano, K., Tobe, H., Morimoto, S., Nagai, T., Yamanaka, T., and Tanaka, M. (1993) Mechanism of pressure-induced amorphization of Ca(OH)₂. *Poton Factory Activity Report*, 11, 201.
- Young, R.A., Prince, F., and Sparks, R.A. (1982) Suggested guidelines for the publication of Rietveld analyses and pattern decomposition studies. *Journal of Applied Crystallography*, 15, 357–359.

MANUSCRIPT RECEIVED MAY 17, 1999

MANUSCRIPT ACCEPTED DECEMBER 1, 1999

PAPER HANDLED BY YANBIN WANG